Proceedings of the ASME 27th International Conference on Offshore Mechanics and Arctic Engineering
OMAE 2008
June 15-20, 2008, Estoril, Portugal

OMAE2008-57171

LINEAR DIFFRACTION AND RADIATION OF SURFACE WAVES BY A HOLLOW SUSPENDED CYLINDRICAL SHELL

Lewis Mitchell
School of Mathematics and Applied Statistics
University of Wollongong
Wollongong, NSW 2500
Australia
Email: lewismitchell1984@gmail.com

Song-Ping Zhu*
School of Mathematics and Applied Statistics
University of Wollongong
Wollongong, NSW 2500
Australia
Email: spz@uow.edu.au

ABSTRACT

A first-order analytical solution for the diffraction and radiation of ocean surface waves around a suspended hollow cylindrical shell is presented. We revisit the problem first studied by Garrett (1970), using a new and more direct technique to obtain the solution for the wave potential. Numerical results are presented for the combined diffraction and radiation problems, showing the wave field inside and around the structure. The results give fundamental insight into both the ideal design and placement of an Oscillating Water Column (OWC) device in the ocean, so as to extract the maximum possible energy from an incident plane wave field.

NOMENCLATURE

a Cylinder radius
d Ocean depth
$\delta_{\beta\alpha}$ Kronecker delta
ε_m $\varepsilon_0 = 1$, otherwise $\varepsilon_m = 2$
g Acceleration due to gravity
H_m m-th order Hankel function of the first kind
I_m m-th order modified Bessel function of the first kind
J_m m-th order ordinary Bessel function of the first kind
K_m m-th order modified Bessel function of the second kind
ω Oscillating surface pressure frequency
P_0 Surface pressure inside cylinder
ϕ Velocity potential of fluid
ρ Fluid density
σ Incoming plane wave frequency
ζ_0 Incoming plane wave amplitude

1 INTRODUCTION

Utilizing renewable energy resources has become an important field of study with regard to combatting climate change. Recent studies show that Oscillating Water Column (OWC) devices are an attractive approach to convert the power of ocean surface waves to electrical energy or to directly use the converted mechanical energy to desalinate water. One example is the wave energy plant at Vizhinjam, Kerala in India [1]. However, to efficiently harness the ocean wave energy, diffraction, refraction and reflection of surface waves around an OWC as well as radiation of waves generated by the turbine attached to an OWC need to be better understood. There is thus renewed research interest in studying wave diffraction around a hollow cylindrical shell structure suspended in an ocean of finite depth.

Two of the problems that arise when trying to design an OWC plant to efficiently extract the maximum energy from an incoming wave field are:

1. how to design the shape of the OWC chamber to extract the largest possible oscillating pressure inside the device, and
2. where to position the device in the ocean to capture waves as large as possible.

*Address all correspondence to this author.

The first point relates to diffraction of incoming plane waves inside the cylinder - we would like to know the optimal design for which the wave elevation inside the cylinder is a maximum, that is for which a wave would resonate and interfere constructively inside the cylinder. The second relates to the combined wave radiation and diffraction by an oscillating surface pressure inside the cylinder - we would like to plot the superimposed radiated and diffracted wave field along with incident plane wave field to fully understand how the OWC structure affects its environment.

Various mathematical treatments of problems relating to OWC devices have appeared in the literature over the years. A fundamental contribution was made by Garrett [2], who solved the first-order diffraction problem for a hollow suspended cylinder in an ocean of constant finite depth. Attempts at solving the radiation problem have been made by Evans [3], who used an unwieldy integral formulation, Evans and Porter [4], who used a numerical method, and Falnes [5], who solved a similar problem to ours, but unlike us focussed more on the calculation of hydrodynamic forces than on the solution for the actual wave field.

In this paper we present an analytical solution for the diffraction and radiation problems for a hollow suspended cylinder in an ocean of constant finite depth, in the form of an infinite series expansion. Solutions of this form are common in physics and engineering [6, 7], and permit numerical calculation to any desired degree of accuracy.

The main difference between our solution and Garrett's lies in the procedure used. Whereas Garrett used a minimization technique to solve the problem, we discovered that it is possible to formulate the problem as a matrix equation, which we solve to obtain the solution directly. This approach has the advantage of requiring less work in analysis than is required by Garrett, and is also computationally easier and more elegant to implement.

In section 2 we formulate the diffraction and radiation problems in terms of an infinite set of simultaneous linear equations, each containing an unknown Fourier coefficient $\mathcal{F}_{m\alpha}$. We show how to solve the system for the unknown $\mathcal{F}_{m\alpha}$'s in section 3, thus obtaining the complete analytic solution for the velocity potential of the fluid at every point in the domain. In section 4 we present our numerical results, with reference to the convergence and accuracy of the solution, and the limitations of the method used. Finally, in section 5 we present our conclusions and discuss further extensions to the theory.

2 PROBLEM FORMULATION

This problem was first solved by Garrett in 1970 [2]. We employ a different method than that used by Garrett to arrive at the numerical solution. We formulate the problem in terms of a system of coupled partial differential equations (PDEs), and use standard separation of variables techniques to obtain an infinite series expansion of the solution. We then use the orthogonality of the eigenfunctions of the system of equations to form a matrix equation which can be solved to any desired level of accuracy for all of the unknown constants in the solution. We treat the diffraction and radiation problems separately, because although the mathematics is similar in both cases, the two problems represent different physical phenomena.

Diffraction Problem

We consider a plane wave of amplitude ζ_0 that is incident upon a hollow cylinder of radius a and zero thickness which is suspended at height h above the floor of an ocean of depth d. The cylinder is fixed to the ocean floor so does not exhibit any rolling or surging motion. A schematic diagram for the diffraction problem is shown in figure 1.

Under a set of standard assumptions [8] for linear water waves, e.g.,

1. incompressible fluid,
2. irrotational flow,
3. inviscid fluid, and
4. small wave amplitude and wavelength ratio (i.e. $\frac{A}{\lambda} << 1$, where A is the amplitude and λ is the wavelength)

the full Navier-Stokes equations reduce to Laplace's equation, subject to a set of linearized boundary conditions. That is, mathematically, we solve

$$\nabla^2\phi = 0, \tag{1}$$

subject to

$$\frac{\partial\phi}{\partial z} = 0 \quad \text{on } z = 0, \tag{2}$$

$$\frac{\partial\phi}{\partial z} - \frac{\sigma^2}{g}\phi = 0 \quad \text{on } z = d, \tag{3}$$

$$\frac{\partial\phi}{\partial r} = 0 \quad \text{on } r = a, \text{ for } h \le z \le d, \tag{4}$$

where ϕ is the velocity potential at a point in the fluid. Here Equation (2) represents a zero flux condition on the ocean floor, (3) is the linearized free surface condition, and (4) represents zero flux on the radial surface of the cylinder. Note that (4) implies that a zero-flux condition has been imposed on both the inner and outer surfaces of the cylinder.

Using the cylindrical symmetry of the problem, we can write ϕ as

$$\phi(r,z,\theta) = \zeta_0 \sum_{m=0}^{\infty} \varepsilon_m i^m \psi_m(r,z)\cos m\theta, \tag{5}$$

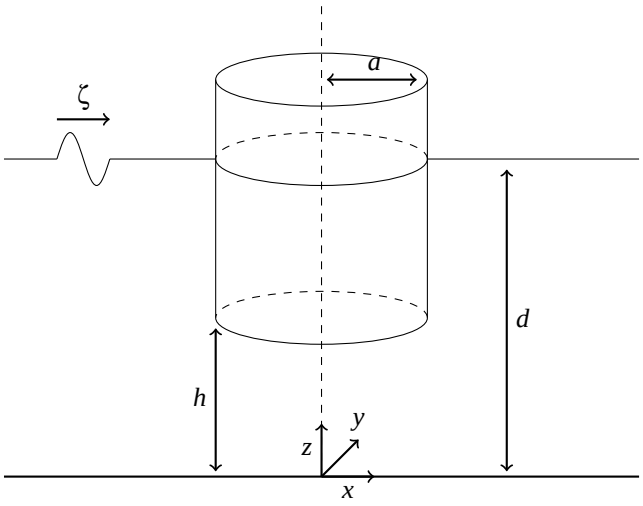

Figure 1. SCHEMATIC DIAGRAM.

and define the surface disturbance ζ as

$$\zeta(r,\theta) = \zeta_0 \sum_{m=0}^{\infty} \varepsilon_m i^m \chi_m(r) \cos m\theta, \tag{6}$$

where χ_m and ψ_m are related by the *kinematic surface condition*, giving

$$\chi_m(r) = \frac{\partial \psi_m}{\partial z}\Big|_{z=d}. \tag{7}$$

We decompose ϕ into two functions defined on $r \le a$ and $r \ge a$ respectively:

$$\phi = \begin{cases} \phi_{int}, & r \le a \\ \phi_{ext}, & r \ge a. \end{cases} \tag{8}$$

In doing this we introduce two continuity conditions at $r = a$:

$$\phi_{int} = \phi_{ext}, \quad \text{and} \tag{9}$$

$$\frac{\partial \phi_{int}}{\partial r} = \frac{\partial \phi_{ext}}{\partial r} \quad \text{for } 0 \le z \le h, \tag{10}$$

which are necessary to close the system.

Solving(1) - (4), we obtain an expansion for the interior potential,

$$\psi_{m,int}(r,z) = \sum_{\alpha} \mathcal{F}_{m\alpha} \frac{I_m(\alpha r)}{\alpha I'_m(\alpha a)} Z_\alpha(z) \tag{11}$$

and similarly we obtain an expansion for the exterior potential,

$$\psi_{m,ext}(r,z) = \left\{ J_m(kr) - \frac{J'_m(ka)}{H'_m(ka)} H_m(kr) \right\} \frac{Z_k(z)}{Z'_k(d)} + \sum_{\alpha} \mathcal{F}_{m\alpha} \frac{K_m(\alpha r)}{\alpha K'_m(\alpha a)} Z_\alpha(z), \tag{12}$$

where k and α are solutions of

$$\sigma^2 - gk \tanh kd = 0 \quad \text{and} \tag{13}$$

$$\sigma^2 + \alpha g \tan \alpha d = 0 \tag{14}$$

respectively. Also,

$$Z_k(z) = N_k^{-\frac{1}{2}} \cosh kz, \tag{15}$$

$$Z_\alpha(z) = N_\alpha^{-\frac{1}{2}} \cos \alpha z, \tag{16}$$

where

$$N_k = \frac{1}{2}\left(1 + \frac{\sinh 2kd}{2kd}\right),$$

$$N_\alpha = \frac{1}{2}\left(1 + \frac{\sin 2\alpha d}{2\alpha d}\right).$$

Kreisel [9] showed that the set $\{Z_k, Z_\alpha\}$, where k and α are given by the dispersion relations (13) and (14) are a complete set of eigenfunctions on the domain $0 \le z \le d$. The $\mathcal{F}_{m\alpha}$'s are then a set of unknown constants to be determined.

Radiation Problem

Mathematically, the radiation of surface waves by an oscillating surface pressure within a hollow suspended cylinder may be considered a dual problem to Garrett's diffraction problem, as the formulation and solution procedure are similar. The physics of the problem however is different to that for diffraction. Whereas in the diffraction problem no energy is generated within the system, the radiation problem involves the continual generation of energy by the oscillating surface pressure within the cylinder, which is carried away by the radiating surface waves. Although this difference is physically important, the formulation for the radiation problem is similar to that of the diffraction problem. The major difference is that the free surface boundary condition (3) is changed to

$$\frac{\partial \phi}{\partial z} - \frac{\omega^2}{g}\phi = \begin{cases} \frac{iP_s}{\rho\omega} & \text{if } r \le a \\ 0 & \text{if } r \ge a \end{cases} \quad \text{on } z = d, \tag{17}$$

where the surface pressure P_s oscillates with simple harmonic motion at frequency ω. As we are not considering transient behavior the radiated waves, only one mode of the excited wave motion is produced, which matches with the mode of the forced oscillation inside the cylinder by this prescribed surface pressure. We will consider a non-uniform pressure distribution, letting

$$P_s(r) = P_0 \cos^2\left(\frac{2\pi r}{a}\right). \tag{18}$$

We transform the problem into Hankel space to obtain the interior solution

$$\psi_{0,int}(r,z) = \frac{i\omega}{\rho} PV \int_0^\infty \frac{\kappa \mathbf{P}(\kappa)\cosh\kappa z J_0(\kappa r)}{\kappa g \sinh\kappa d - \omega^2\cosh\kappa d} d\kappa + \frac{k\mathbf{P}(k)\cosh kz J_0(kr)}{g\sinh kd + kdg\cosh kd - \omega^2 d\sinh kd}, \tag{19}$$

where $\mathbf{P}(\kappa)$ is the Hankel transform of P_0,

$$\mathbf{P}(\kappa) = \int_0^a r P_s(r) J_0(\kappa r) dr,$$

and PV represents a Cauchy principal value integral. We find that $\psi_{m,int} = 0$ for all $m > 0$, and the exterior expansion is the same as for the diffraction problem.

3 SOLUTION

The solution for both the diffraction and radiation problems involves using the orthogonality of the eigenfunctions $Z_\alpha(z)$ on the domain $0 \le z \le d$. Substituting the interior and exterior expansions for ψ into the continuity condition (9) and integrating over the domain $0 \le z \le d$, we obtain a matrix equation:

$$\mathbf{E}_{\beta\alpha}\mathcal{F}_{m\alpha} = F_m \mathbf{C}_\beta \tag{20}$$

for the diffraction problem, where

$$F_m = 2i\left[\pi k a^2 H_m'(ka) Z_k'(d)\right]^{-1}, \tag{21}$$

$$R_\alpha = \left[\alpha^2 a^2 I_m'(\alpha a) K_m'(\alpha a)\right]^{-1}, \tag{22}$$

$$C_\beta = \frac{1}{d}\int_0^h Z_k(z) Z_\beta(z) dz, \tag{23}$$

$$D_{\beta\alpha} = \frac{1}{d}\int_0^h Z_\alpha(z) Z_\beta(z) dz, \tag{24}$$

$$E_{\beta\alpha} = (R_\alpha - 1) D_{\beta\alpha} + \delta_{\beta\alpha}. \tag{25}$$

We obtain a similar expression for the radiation problem:

$$\mathbf{E}_{\beta\alpha}\mathcal{F}_{1m\alpha} = \mathbf{F}_\beta, \tag{26}$$

where

$$F_\beta = \frac{i\omega}{\rho d} PV \int_0^\infty \frac{\kappa \mathbf{P}(\kappa) J_0(\kappa a)}{\kappa g \sinh\kappa d - \omega^2\cosh\kappa d} \int_0^h \cosh\kappa z Z_\beta(z) dz d\kappa + \frac{k\mathbf{P}(k) J_0(ka) N_k^{1/2}}{g\sinh kd + kdg\cosh kd - \omega^2 d\sinh kd} C_\beta, \tag{27}$$

$$E_{\beta\alpha} = (R_\alpha - 1) D_{\beta\alpha} + \delta_{\beta\alpha}, \tag{28}$$

$$R_\alpha = \frac{K_m(\alpha a)}{\alpha K_m'(\alpha a)}. \tag{29}$$

The solution of the matrix equations (20) and (26) give the complete series solution for the fluid potential ϕ on the whole domain. For computational purposes we truncate the series over m after M terms and the series over α after N terms. Then $\mathbf{E}_{\beta\alpha}$ is an $N \times N$ matrix, $\mathcal{F}_{m\alpha}$ is a vector with N elements, F_m is a scalar which depends upon m, and C_β as another vector with N elements. Solving this matrix equation for the unknown $\mathcal{F}_{m\alpha}$ we obtain the solution for ϕ on the whole domain, $r \le a$ and $r \ge a$.

4 RESULTS

In analysing our solution there are three important issues to consider:

1. rate of convergence of the series solution,
2. agreement with previous numerical results and experiments, and
3. how well the boundary conditions are satisfied by the solution.

We examine each of these for the diffraction and radiation problems. Unless otherwise indicated, we use the parameter values $g = 9.8$ ms^{-1}, $P_0 = 100$ Pa, $\sigma = 1.2$ s^{-1}, $\rho = 1$ kgm^{-3} and $\zeta_0 = 1$ m in the following numerical examples. Figure 2 shows a surface wave elevation profile for the diffraction problem for a range of values of m, demonstrating that the solution converges quickly with m. Figure 3 shows the convergence of the solution by measuring the difference between consecutive terms $||\zeta_n - \zeta_{n-1}||$, where the norm is defined by

$$||\zeta_n|| = \sum_{m=0}^{n} \varepsilon_m i^m \sum_{r=0}^{R} \chi_m(r)\cos m\theta.$$

Here R is an arbitrary distance from the cylinder, which we choose as $7a$ in our numerical examples, and the norm measures the first n partial sums of the series solution.

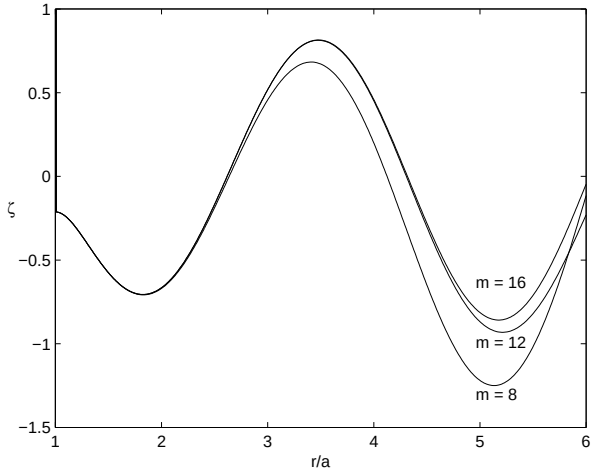

Figure 2. SURFACE DISPLACEMENT ALONG $\theta = 0$ FOR $a = 10$ m, $d/a = 0.6$, $h/a = 0.4$.

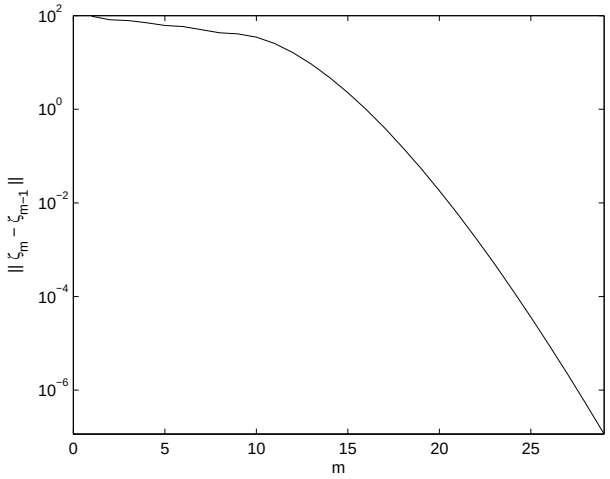

Figure 3. ERROR $||\zeta_m - \zeta_{m-1}||$ AS A FUNCTION OF m, for $a = 10$ m.

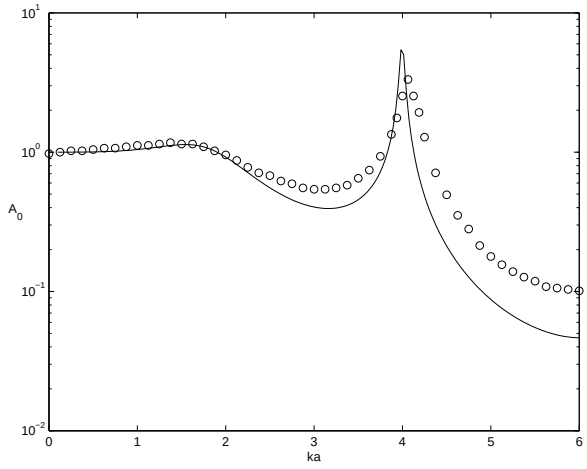

(a) $h/a = 0.4$.

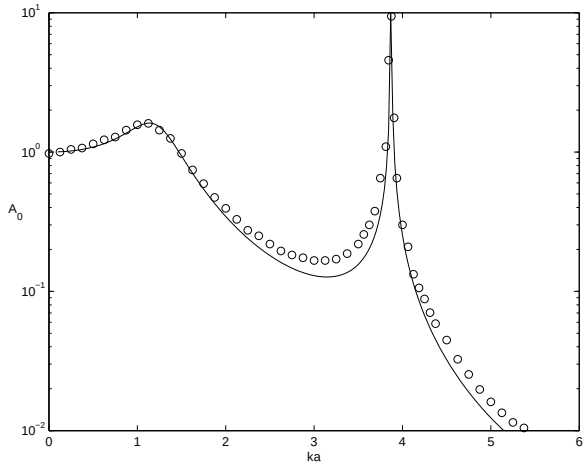

(b) $h/a = 0.2$.

Figure 4. NUMERICAL COMPARISON OF INTERNAL WAVE AMPLITUDES FOR $m = 0$, $d/a = 0.6$. SOLID LINE IS OUR SOLUTION, DOTS ARE GARRETT'S SOLUTION.

Figure 4 shows a comparison between our solution (solid line) and Garrett's solution (dots) for two different cylinder geometries. The function being plotted is

$$A_m = \mathcal{F}_{mk} \frac{Z_k'(d)}{kJ_m'(ka)}, \tag{30}$$

for $m = 0$, and represents the first term in the expansion of the wave amplitude inside the cylinder. Numerically and physically, this is the most important term in the solution. As the figures show, our solution generally agrees well with Garrett's. Also, the fit is better for $h/a = 0.2$ than for $h/a = 0.4$. We believe this is an indication of how well the boundary condition is satisfied at $r = a$. Overall, our numerical experiments show good agreement with Garrett's results, and are more than sufficient for practical purposes.

To demonstrate how well our series solution satisfies each of the three boundary conditions we examine how close each of the functions in equations (2) - (4) are to zero. The first two boundary conditions (2) and (3) are exactly satisfied, so the only boundary condition of interest to study is (4).

Figure 5 shows $\frac{\partial \psi_m}{\partial r}$ as a function of z for $r = a$. That is, the figure shows how well the solution matches the boundary condition (4) for different values of m. The figures show that the solution converges quickly, but figure 5(b) in particular shows that (4) is not perfectly satisfied for $h \leq z \leq d$. This is due to Gibbs phenomenon, which occurs when trying to use a Fourier series to describe a function with a discontinuity, as happens here at $r = a$ and $z = h$. The effect of this singularity however is decreased as the cylinder submergence is increased - figure 6 shows an example of how the error in matching the boundary condition (4) depends on the cylinder submersion, by defining a norm of the error per unit submergence depth

$$\left|\left|\frac{\partial \psi_m}{\partial r}\right|\right| = \frac{\sum_{z\in[h,d]} \left|\frac{\partial \psi(a,z)}{\partial r}\right| \Delta h}{d-h},$$

where Δh is a small height increment, and plotting it as a function of h/a. In general the solution is more accurate for deeper submergence, but figure 5(b) shows that even for shallow submergence the results are at worst less than $O(1)$. We thus conclude that Gibbs phenomenon only poses an issue for extremely shallow submergence depths, so in general the singularity at $z = d$ has only a minor effect upon the solution.

Finally, we present surface wave plots for the diffraction and radiation problems. Figures 7 and 8 show some representative wave height contour plots for the diffraction problem. Figure 7 shows the diffracted wave only outside the cylinder, not the incoming plane wave. Similarly, figure 8 shows the diffracted wave heights only inside the hollow cylinder. Figures such as this provide information about the relationship between cylinder radius (and submersion) and wave elevation, as well as the non-uniformity of the wave inside the cylinder.

Figure 9 shows a surface profile for the radiation problem, using $P(r) = P_0 \cos^2\left(\frac{2\pi r}{a}\right)$. As the pressure distribution used is θ - independent, the radiated wave heights will be as in the surface profile figure in every direction around the cylinder. The complete surface profile, incorporating the combined diffraction and radiation effects, is the linear superposition of the two relevant plots, figures 7 and 9. A superposition such as this provides information about how the cylindrical structure affects its environment in a plane surface wave field.

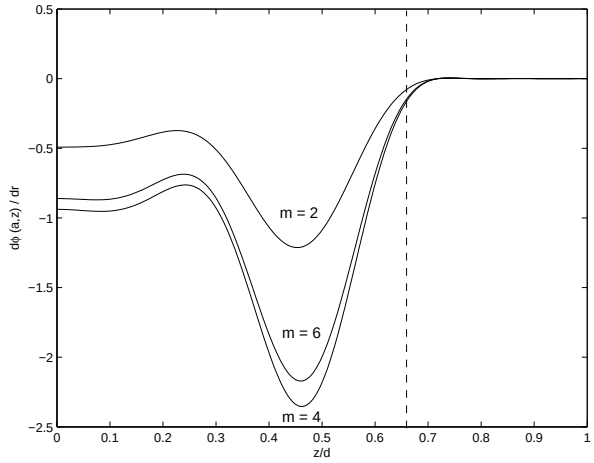

(a) $a = 10$ m.

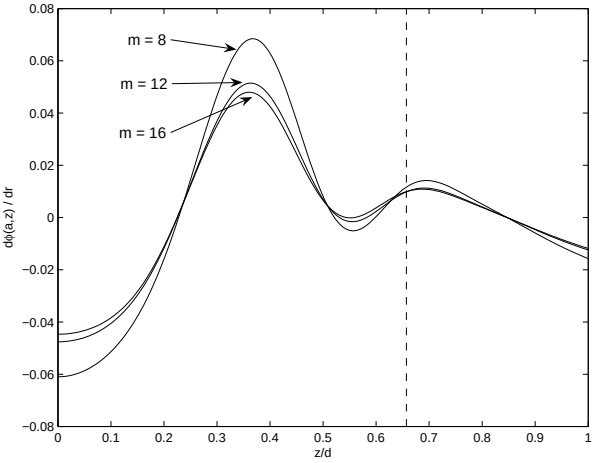

(b) $a = 60$ m.

Figure 5. $\frac{\partial \phi}{\partial r}$ AS A FUNCTION OF z, DIFFERENT VALUES OF m.

5 CONCLUSIONS

This analysis has allowed us to obtain fundamental insights into how the excited waves inside of a hollow structure such as an OWC device would behave. By focussing our study on analytic solutions, we obtained an exact solution for the diffraction and radiation problems of a suspended hollow cylinder in an ocean of finite depth. This is important in the study of actual OWC devices, as a fundamental basis for the theory of more complicated structures. In particular, this work will be useful for later numerical modelling of OWC structures, as a tool for verifying the validity of a particular numerical scheme. This work then represents a first step towards a more complete model of a real OWC device.

REFERENCES

[1] Sharmila, N., Jalihal, P., Swamy, A. K., and Ravindran, M., 2004. "Wave powered desalination system". *Energy*, **29**(11), pp. 1659–1672.

[2] Garrett, C. J. R., 1970. "Bottomless harbours". *J. Fl. Mech*,

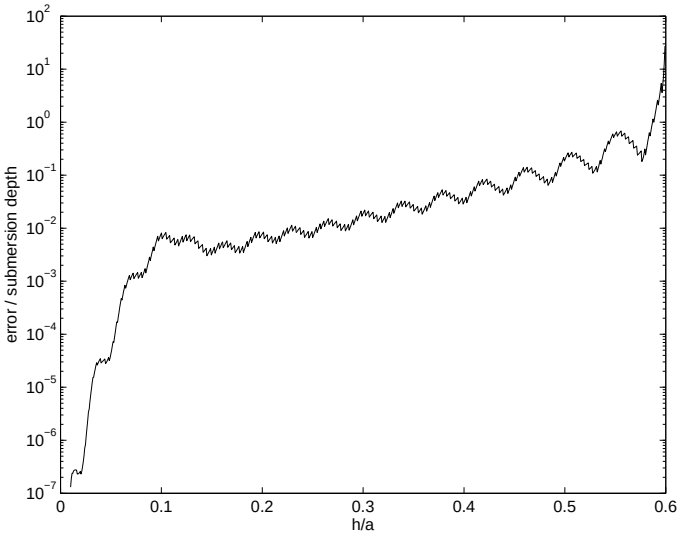

Figure 6. BOUNDARY CONDTITION MATCHING ERROR OVER SUBMERSION DEPTH AS A FUNCTION OF h/a, $a = 10$.

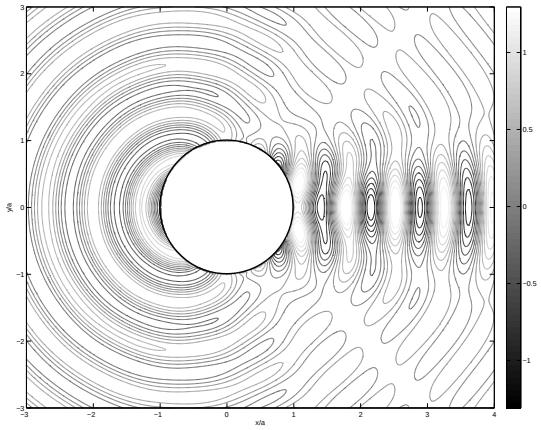

Figure 7. CONTOUR PLOT SHOWING DIFFRACTED WAVE ELEVATION $a = 60$ m.

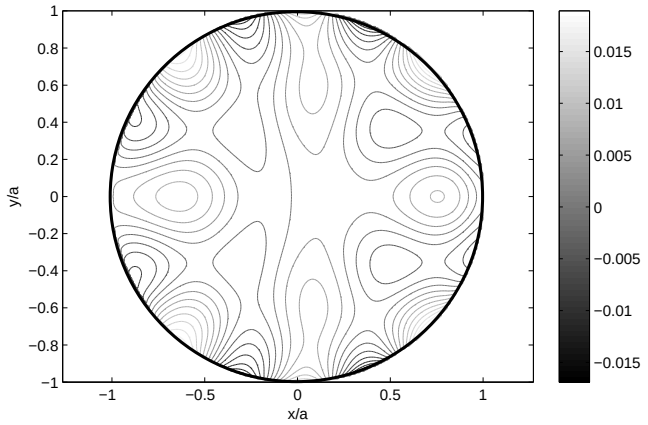

Figure 8. CONTOUR PLOT SHOWING WAVE ELEVATION INSIDE CYLINDER FOR $a = 60$ m.

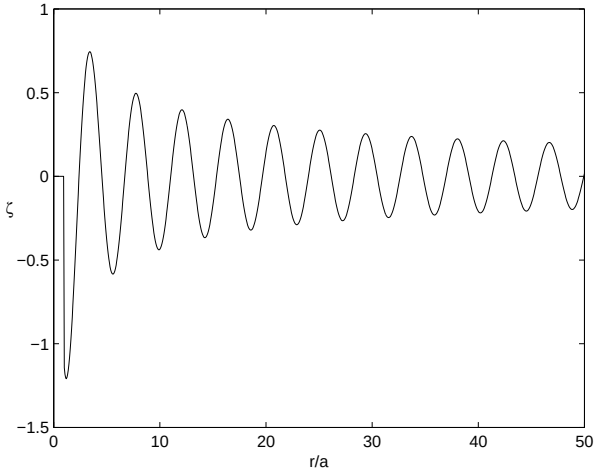

Figure 9. RADIATED WAVE PROFILE ALONG $\theta = 0$.

43(3), pp. 433–449.

[3] Evans, D. V., 1982. "Wave-power absorption by systems of oscillating surface pressure distributions". *J. Fl. Mech,* **114**, pp. 481–499.

[4] Evans, D. V., and Porter, R., 1997. "Efficient calculation of hydrodynamic properties of owc-type devices". *J. Offshore Mech. and Arctic Engng.*, **119**(4), pp. 210–218.

[5] Falnes, J., 2002. *Ocean Waves and Oscillating Systems.* Cambridge University Press, New York.

[6] Carslaw, H. S., and Jaeger, J. C., 1959. *Conduction of Heat in Solids.* Clarendon Press, Oxford.

[7] Hildebrand, F. B., 1976. *Advanced Calculus and Applications.* Prentice-Hall, Englewood Cliffs, NJ.

[8] Mei, C. C., 1989. *The Applied Dynamics of Ocean Surface Waves.* World Scientific, Singapore.

[9] Kreisel, G., 1949. "Surface waves". *Q. Appl. Math.*, **7**, pp. 21–24.